ACS OMEGA
http://pubs.acs.org/journal/acsodf
Article

Electromagnetic Interference Shields Based on Highly Crystalline Single-Walled Carbon Nanotubes

Norihiro Shimoi,* Masae Komatsu, and Masayoshi Isago

Cite This: ACS Omega 2024, 9, 29009–29016
Read Online

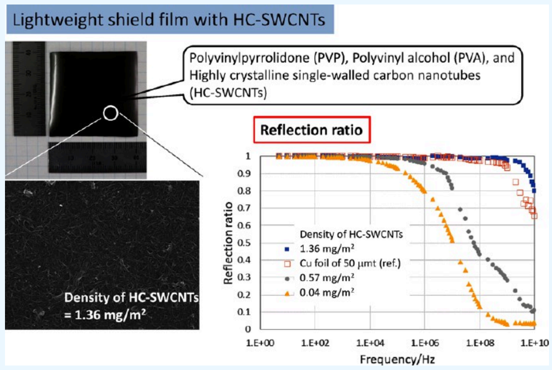

ABSTRACT: Although the convenience provided by electromagnetic waves used for information exchange is increasing, the energy of unwanted electromagnetic waves unintentionally emitted from devices is increasing as the devices work with higher frequency. In view of this vulnerability, thin films as lightweight electromagnetic wave shields against noise will be necessary for information protection. We propose the fabrication of lightweight electromagnetic wave shields using highly crystalline single-walled carbon nanotubes (HC-SWCNTs), which can be made large and flexible using a method based on a wet process, utilizing the optical and conductive properties of HC-SWCNTs. Electromagnetic wave shields are mainly classified into conductive, dielectric, and magnetic absorbers. We have developed a material synthesis technology for HC-SWCNTs and attempted to form an aqueous composite film using HC-SWCNTs and an organic binder. As a result, we found that the high crystallinity of CNTs suppresses the contact resistance between CNTs and we succeeded in constructing a flexible electromagnetic wave shielding film that can absorb electromagnetic waves in a wide bandwidth equivalent or superior to that of metal foil. This thin film can be applied to curved surfaces as desired because of its wet process, and it is expected to be a lightweight shield that can be used ubiquitously.

INTRODUCTION

The IoT society has recently come owing to the marked increase in the amount of digital data and the expansion of cyberspace associated with the development of information and communication technology (ICT). The creation of platforms that integrate cyberspace and real space has become essential, and the emergence of advanced devices that stably handle huge amounts of data, especially in real space, is predicted. On the other hand, there is a need for a technology that reduces the environmental impact of fabrication processes on a global scale. Taking these global technology issues into consideration, we have been considering how functional electronic materials can be prepared for device fabrication in the IoT society on the basis of the results of our research to date.

Wireless technology is used for the construction of networks for exchanging information between systems in real space, and there are several standards for wireless technology for sharing information, such as Wi-Fi, which is essential. In such a technology, a heavy electromagnetic wave absorber is necessary to prevent information transmission deficiencies due to radio wave information interference and confusion, prevent unintended interception by security systems, and protect information. Heavy absorbers are necessary for information protection but are difficult to use ubiquitously in all environments. Considering the advent of the IoT society and to satisfy data ubiquity and the flexibility of devices that transfer and receive radio waves, an electromagnetic wave absorber must be lightweight and continuity and flexibility are essential specifications for materials used as membranes to absorb electromagnetic waves.

Dielectrics and conductors are commonly used as materials for electromagnetic wave shields.[1−5] The synthesis of fine particles of metals used to form thin, lightweight, and flexible electromagnetic shields that protect electrical devices from electromagnetic waves has been reported by many research and development organizations, mainly on synthesis methods for precious metals such as silver, platinum, and copper. A synthesis method based on noble metal nanoparticle synthesis processes is expensive and the contact resistance between metal nanoparticles hinders shielding against electromagnetic waves. To form thin and lightweight electromagnetic shields, we developed and synthesized a composite material with an organic binder using carbon nanomaterials. Carbon materials

Received: May 5, 2024
Revised: June 4, 2024
Accepted: June 11, 2024
Published: June 18, 2024

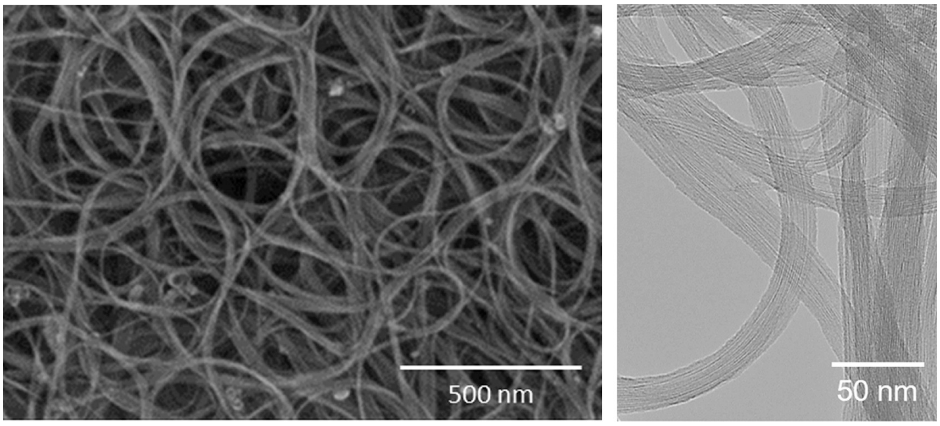

Figure 1. (Left) SEM and (right) TEM images of SWCNTs synthesized by arc discharge and annealing at 1200 K and 10^{-5} Pa.

are generally used as absorbers of high-bandwidth electromagnetic waves, but most of them have an amorphous crystalline structure. We have been focusing on carbon nanotubes (CNTs) as a carbon material and applied them to electromagnetic shielding. There are many reports on the electromagnetic properties of thin films formed by CNTs alone or mixed with other organic or conductive materials, and they showed electromagnetic shielding properties equivalent to metal foils in the frequency range from MHz to above GHz. The formation of CNT films with electromagnetic shielding properties equivalent to those of metallic foils or nanowires in the frequency range from MHz to GHz and above has not been reported. The electrical conductivity of CNT films significantly affects the absorption of electromagnetic waves in the high-frequency range, but it is assumed that the electrical conductivity of CNTs with crystal defects makes it difficult to shield electromagnetic waves in the high-frequency range. We have successfully synthesized highly crystalline single-wall carbon nanotubes (HC-SWCNTs) with almost no crystal defects[6−9] and experimentally confirmed that their electrical properties are close to theoretically derived properties.[10−14] HC-SWCNTs, which exhibit almost no crystal defect breaks in the carbon network comprising CNTs, show almost no energy loss and have a high mobility of more than 1000 $cm^2/V{\cdot}s$. Despite their tubular crystalline structure, the presence of randomly oriented HC-SWCNTs in films is expected to make their electrical conductivity comparable to that of bulk carbon materials such as graphite and bulk metals.[6] Furthermore, in terms of specific gravity, they are expected to perform similarly to bulk carbon in very small quantities. We have successfully synthesized HC-SWCNTs with high purity and reported the synthesis method.[6,7,9] On the basis of the developed nanotube synthesis method, we set out to form buckypaper made of nanotube powder, which is convenient for thin-film formation to ensure conductivity between nanomaterials, and the formation of the HC-SWCNT thin film is expected to be cost-effective, large-area, and flexible.

In this paper, we report the results of our attempts to fabricate lightweight electromagnetic wave shields using HC-SWCNTs by a wet process and to evaluate their electromagnetic wave shielding properties.

■ EXPERIMENTAL PROCEDURE

The HC-SWCNTs used in this study were synthesized from soot containing about 10 wt % CNTs by arc discharge in a carbon electrode with catalytic metals. After collecting the soot, catalytic metal nanoparticles, nanocarbon particles, and amorphous carbon particles, which were produced simultaneously as byproducts, were removed by a purification process.[11,15,16] First, all the different composites were separated into individual products by hydrothermal treatment. Then, low-temperature calcination was conducted to remove amorphous carbon, followed by acid dissolution and the removal of metal nanoparticles. Finally, nanocarbon and capsule particles and CNTs were separated using gravity to obtain high-purity CNTs. The purity of the resulting CNTs was found to be approximately 97% by inductively coupled plasma analysis[17] and differential thermal analysis.[9] A small number of catalytic metal nanoparticles remain in the sample, which cannot be identified by electron microscopy. Annealing the SWCNTs at a high temperature of 1200 K and a high vacuum of 10^{-5} Pa produced HC-SWCNTs. The SEM and TEM images of HC-SWCNTs after annealing are shown in Figure 1.

HC-SWCNT solution dispersed with ethylcellulose as a surfactant in a jet mill was subjected to suction filtration to obtain only CNTs. After vacuum drying at 130 °C, the formed paper-like CNT film was peeled off from the filter paper. The CNT film of about 50 μm thickness consisted of only HC-SWCNTs, and its imaginary susceptibility and reflection coefficiency for electromagnetic radiation were measured. In addition, for comparison, sheets of buckypaper were also prepared using commercial SWCNTs containing crystalline defects and their parameters for electromagnetic radiation were verified.

A photograph and magnified surface SEM images of the buckypaper made of HC-SWCNTs and dried state after suction filtration are shown in Figure 2.

In this study, to reduce the weight of electromagnetic wave shields and to form a large-area film with electromagnetic wave

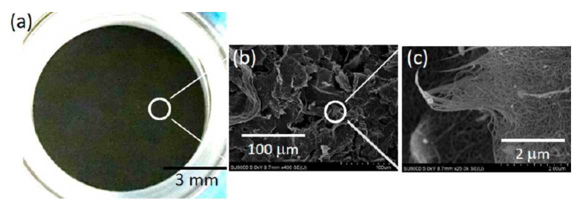

Figure 2. Buckypaper composed of only HC-SWCNTs. (a) Photograph, (b) SEM image, and (c) magnified SEM images of surface of HC-SWCNT buckypaper.

https://doi.org/10.1021/acsomega.4c04285
ACS Omega 2024, 9, 29009−29016

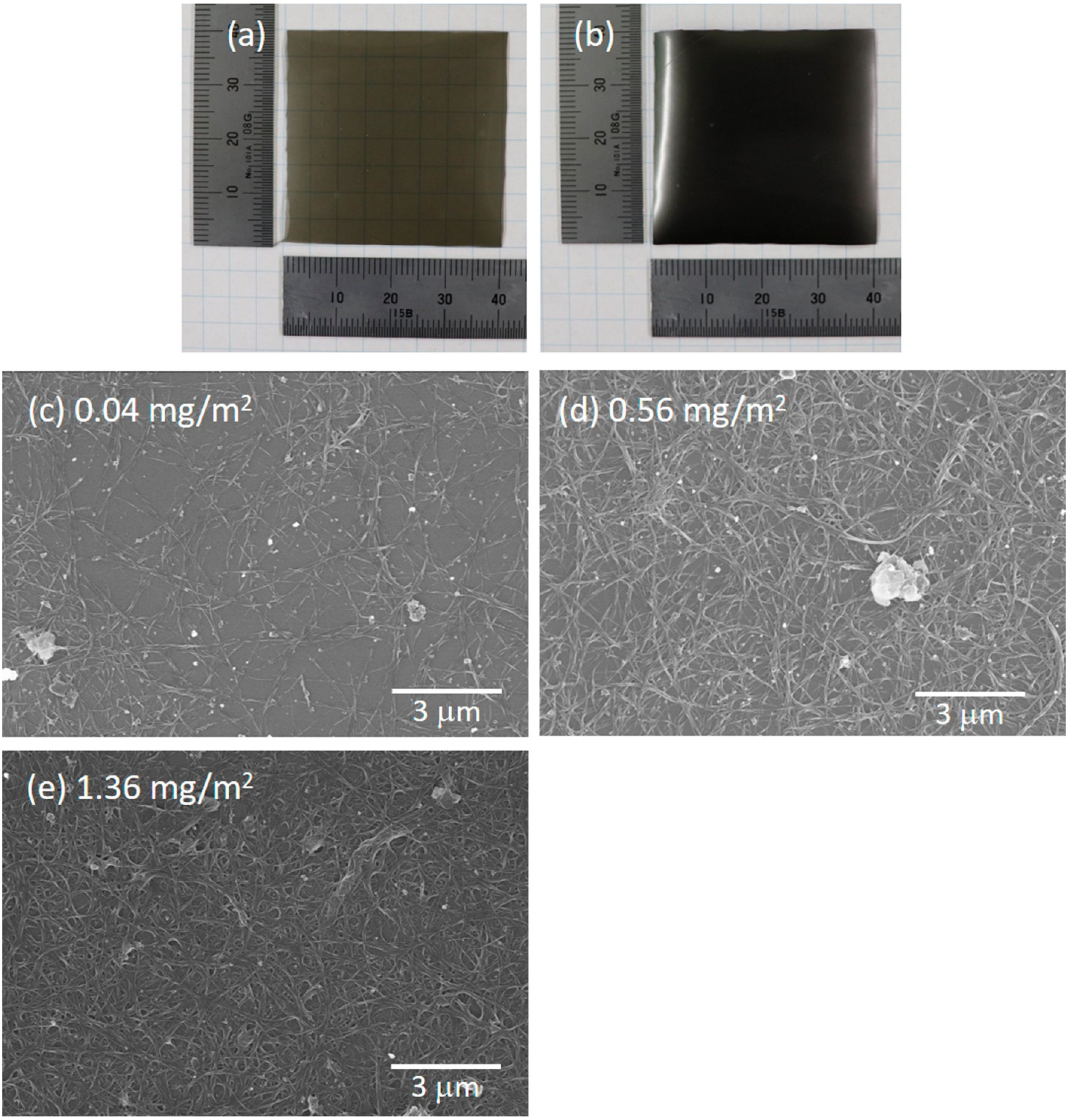

Figure 3. (a, b) Photographs of composite films with PVP and HC-SWCNTs added at densities of 0.56 and 1.36 mg/m^2, respectively. (c−e) SEM images of film surfaces with HC-SWCNTs added at densities of 0.04, 0.56, and 1.36 mg/m^2, respectively.

shielding properties, an HC-SWCNT dispersion was mixed with polyvinylpyrrolidone (PVP), isopropyl alcohol (IPA), citric acid, and poly(vinyl alcohol) (PVA) in water to form composite films with organic binders. CNT dispersion aqueous solutions were prepared, with the density of HC-SWCNTs added per unit area arbitrarily adjusted, and the solutions were uniformly spread on a hot plate at 130 °C using an applicator to form films with a thickness of 100 μm. The formed films were further dried on the hot plate. Photographs and SEM images of the HC-SWCNT films after their formation and film surfaces at various densities of HC-SWCNTs added are shown in Figure 3. The dielectric constant and electromagnetic shielding properties of the samples were evaluated in this experiment.

An impedance analyzer (E4991A, Agilent Co., Ltd.) was used in this study to evaluate the dielectric constant. The frequency range was evaluated over a high bandwidth from 1 M to 10 GHz. A sample was regarded as a homogeneous bulk body, and the dielectric constant was evaluated from the impedance Z of the concentrated constant equivalent circuit shown in Figure 4. The optical constants were estimated from the complex dielectric, and the electromagnetic shielding

https://doi.org/10.1021/acsomega.4c04285
ACS Omega 2024, 9, 29009−29016

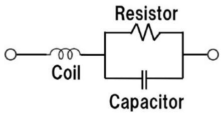

Figure 4. Equivalent circuit for measuring the dielectric constant of sample films for electromagnetic shielding.

properties were calculated from the optical absorption coefficient (α) and reflectance (R). The samples were evaluated for their electricity flow in bulk as a conductive property.

The dielectric properties of the samples were extracted from the data obtained with an impedance analyzer by calculating eqs 1−3.

$$\varepsilon_r' = \frac{d}{\omega\varepsilon_0 S}\frac{\omega L - \mathrm{Im}(Z)}{(\omega L - \mathrm{Im}(Z))^2 + \mathrm{Re}(Z)^2} \tag{1}$$

$$\varepsilon_r'' = \frac{d}{\omega\varepsilon_0 S}\frac{\mathrm{Re}(Z)}{(\omega L - \mathrm{Im}(Z))^2 + \mathrm{Re}(Z)^2} \tag{2}$$

$$L = \frac{\left(\frac{\mathrm{Im}(Z)}{\partial\omega}\right)^2 + \left(\frac{\mathrm{Re}(Z)}{\partial\omega}\right)^2}{2\frac{\partial \mathrm{Im}(Z)}{\partial\omega}} \tag{3}$$

■ RESULTS AND DISCUSSION

Figure 5 shows the complex permittivity of the sheets of buckypaper formed with SWCNTs containing crystal defects

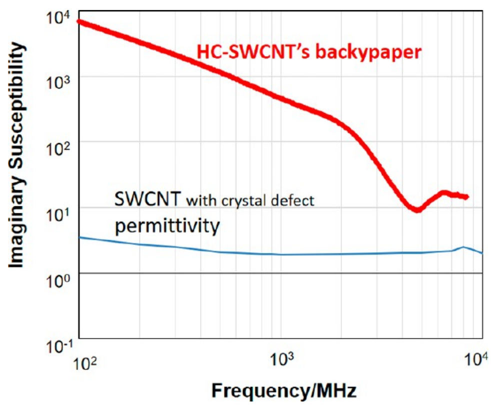

Figure 5. Frequency dependence of complex permittivity (imaginary part) of HC-SWCNT buckypaper and buckypaper formed with SWCNTs with crystal defects.

and HC-SWCNTs. Whereas the imaginary part of the complex permittivity of the buckypaper formed with commercial SWCNTs containing defects was around 5−10, that of the HC-SWCNT buckypaper was found to be 100−1000 in the GHz band and to have optical properties. Therefore, a PVA composite film was formed using HC-SWCNTs and we evaluated its electromagnetic wave absorption property in the relevant range.

Dielectrics and conductors are used as materials for electromagnetic wave shields, and carbon materials are generally utilized as absorbers of high-bandwidth electromagnetic waves, but the carbon used as the conductive additive in a shield film is mostly an amorphous material. We have confirmed that the HC-SWCNTs used in this study exhibit physical properties close to their theoretical properties, and we expect improvement in their properties when used as an additive in such shielding membranes. In particular, the imaginary part of the complex dielectric constant is more than one digit larger depending on the presence or absence of crystal defects. Moreover, as shown in Figure 5, HC-SWCNT buckypaper is expected to have beneficial properties for electromagnetic wave absorption at high frequencies as a dielectric electromagnetic absorber.[18−20] This suggests that optical properties of HC-SWCNT buckypaper equivalent to or higher than those of bulk carbon such as graphite can be obtained despite the tubular crystal structure. Furthermore, in terms of specific gravity, HC-SWCNT buckypaper is expected to have properties equivalent to those of bulk carbon in very small quantities.

When the frequency dependence of the reflection property of buckypaper with a diameter of 10 mm and a thickness of 0.05 mm composed of HC-SWCNTs was verified, a maximum electromagnetic wave shielding of −18.3 dB at 0.08 GHz was successfully measured in the measurement bandwidth range of 2 kHz to 0.1 GHz. This suggests the possibility of the highly efficient absorption of electromagnetic waves in the GHz band, as shown in Figure 6.

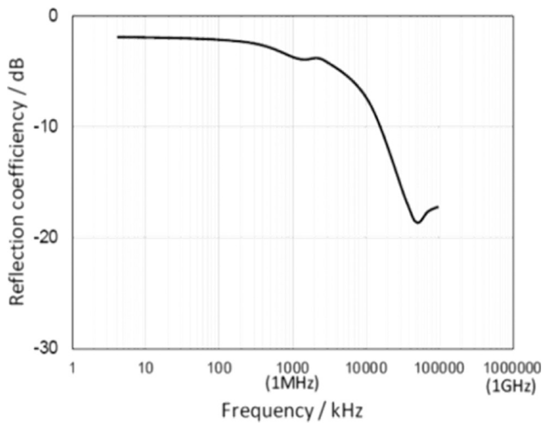

Figure 6. Electromagnetic wave reflection property of HC-SWCNT buckypaper (10 mm diameter, 0.05 mm thickness). Measurement bandwidth range: 2 kHz to 0.1 GHz.

Furthermore, the dielectric (Figure 7), absorption (Figure 8), and reflection (Figure 9) properties of the composite films with HC-SWCNTs, PVP, PAP, and IPA were evaluated by calculating each parameter using eqs 1−3 and considering the results of the complex impedance evaluation. In this study, the density of HC-SWCNTs added to each thin film was evaluated for samples adjusted to 1.36, 0.57, and 0.04 mg/m^2, and a copper thin film of 50 μm thickness was used as reference.

From these results, it is clear that CNT composite films formed above a certain density have potential applications as electromagnetic shields with properties equivalent or superior to those of bulk materials such as copper foil. From the above, the control of the frequency band and the optimization of the electromagnetic wave absorption property by utilizing the high-frequency properties of HC-SWCNTs were realized through the formation of composite films composed of HC-SWCNTs, PVP, IPA, and PVA, and by controlling the density of HC-SWCNTs added.

Ideal SWCNTs have high theoretical mobilities of around 5000−10,000 cm^2/(V s).[21−26] On the other hand, in CNT

https://doi.org/10.1021/acsomega.4c04285
ACS Omega 2024, 9, 29009−29016

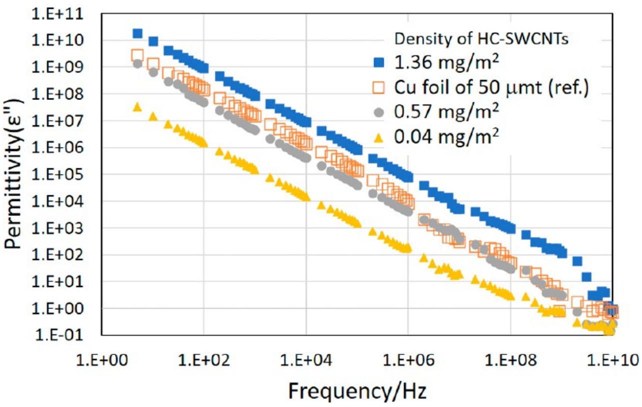

Figure 7. Dielectric property of films with controlled CNT addition and copper foil as a reference. The density of HC-SWCNT in each film was adjusted to 1.36, 0.57, and 0.04 mg/m^2, respectively.

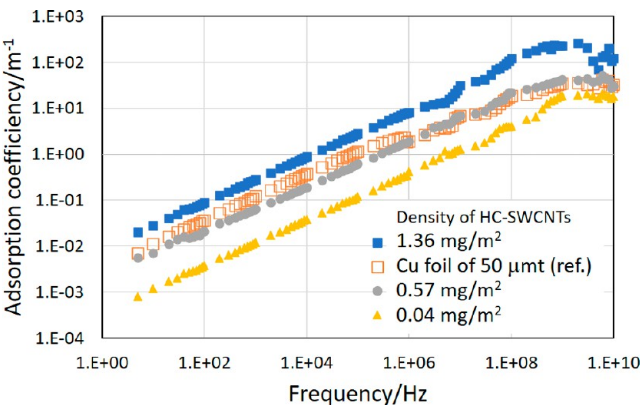

Figure 8. Absorption property of HC-SWCNT composite films and Cu foil.

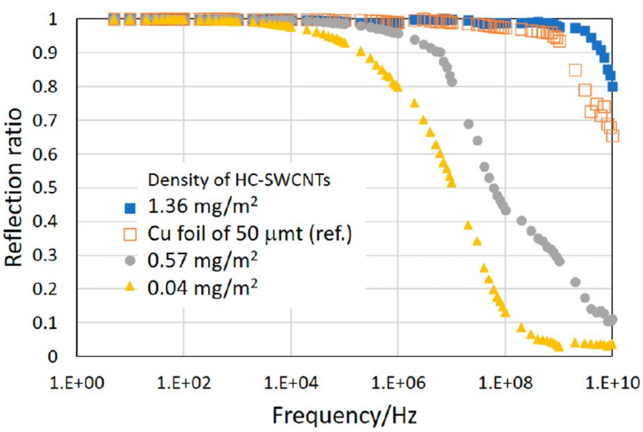

Figure 9. Reflection property of HC-SWCNT composite films and Cu foil.

films formed by the wet process, there is electrical resistance due to contact points between CNTs, as a number of CNTs are folded in a mesh pattern, as shown in Figure 3. The conduction property of the entire membrane evaluated in this study is considered to originate from the magnitude of the electrical resistance due to contact points between CNTs. To analyze the results shown in Figures 6–9, the significant difference in contact resistance due to the crystallinity of SWCNTs was evaluated in this study. CNTs were suitably dispersed on a Ta substrate, and the contact resistance was evaluated by scanning probe microscopy (SPM, MultiMode 8-PeakForce TUNA (tunneling AFM), Bruker Corporation) to measure tunneling current. An arbitrary voltage was applied between the sample and the probe, and the current flowing in the circuit was detected.

In this study, a platinum–iridium-coated tip attached to a silicon nitride-based cantilever, which has a spring constant of 0.4 N/m, was used as the SPM probe. The measurement conditions were the same for all samples (Table 1).

Table 1. SPM Measurement Conditions

measurement area	1 μm × 1 μm
scan rate	0.18–0.20 Hz
amplitude set point	250 mV
drive amplitude	750–825 mV
DC bias	1.5 V

We prepared samples of SWCNTs dispersed in acetone and then dried by heat volatilization at 150 °C on a Ta substrate. 3D images of an SWCNT bundle and images of the current distribution at the same location are shown in Figure 10. Figure 10a,b shows HC-SWCNTs, and Figure 10c,d shows SWCNTs with crystal defects. In the current distribution image, the dark-brown area is where the current was detected and the shape of the CNTs can be discerned. In the area where current was detected, SWCNTs with crystal defects appear discontinuous compared with HC-SWCNTs and there are several areas where the current did not flow uniformly. Furthermore, contact resistance develops where CNTs or CNT bundles come into contact with each other, and especially at contact points between SWCNTs with crystal defects, the contact resistance is high and current cannot be detected in many places. Therefore, a graph showing the current–voltage characteristics of the arbitrarily selected intersection points of each sample is shown in Figure 11. The measurement points A–F are indicated by arrows in Figure 10b,d. It is assumed that the SWCNTs with crystal defects have a relatively higher resistance and that the uneven internal resistance of the CNTs makes it difficult for current to flow owing to the high internal resistance between adjacent CNTs. From the voltage–current characteristics of each sample, the contact resistance can be approximated and the magnitude of contact resistance depending on the crystallinity of SWCNTs can be determined. From the above results, it was found that the current flowing in SWCNTs depends on the crystallinity of the SWCNTs.

From the above results, it was found that the charge mobility is markedly improved by the percolation effect due to the density and crystallinity of the SWCNTs added. This can be explained by the following findings. The number of contact points of SWCNTs can be increased or decreased by controlling the density of SWCNTs added, and the contact resistance between SWCNTs and the resistivity inside SWCNTs change depending on the crystallinity, which is reflected in charge mobility.[27−31] The contact resistance of HC-SWCNTs is generally low when each CNT is in contact with another CNT. It is assumed that the density and arrangement of CNTs improve the conduction property of the film through the formation of the shortest path for charges to pass through multiple contact points attributable to the percolation effect.[32−34] However, if the SWCNTs contain crystal defects, it is difficult to form a path for charges to pass

https://doi.org/10.1021/acsomega.4c04285
ACS Omega 2024, 9, 29009−29016

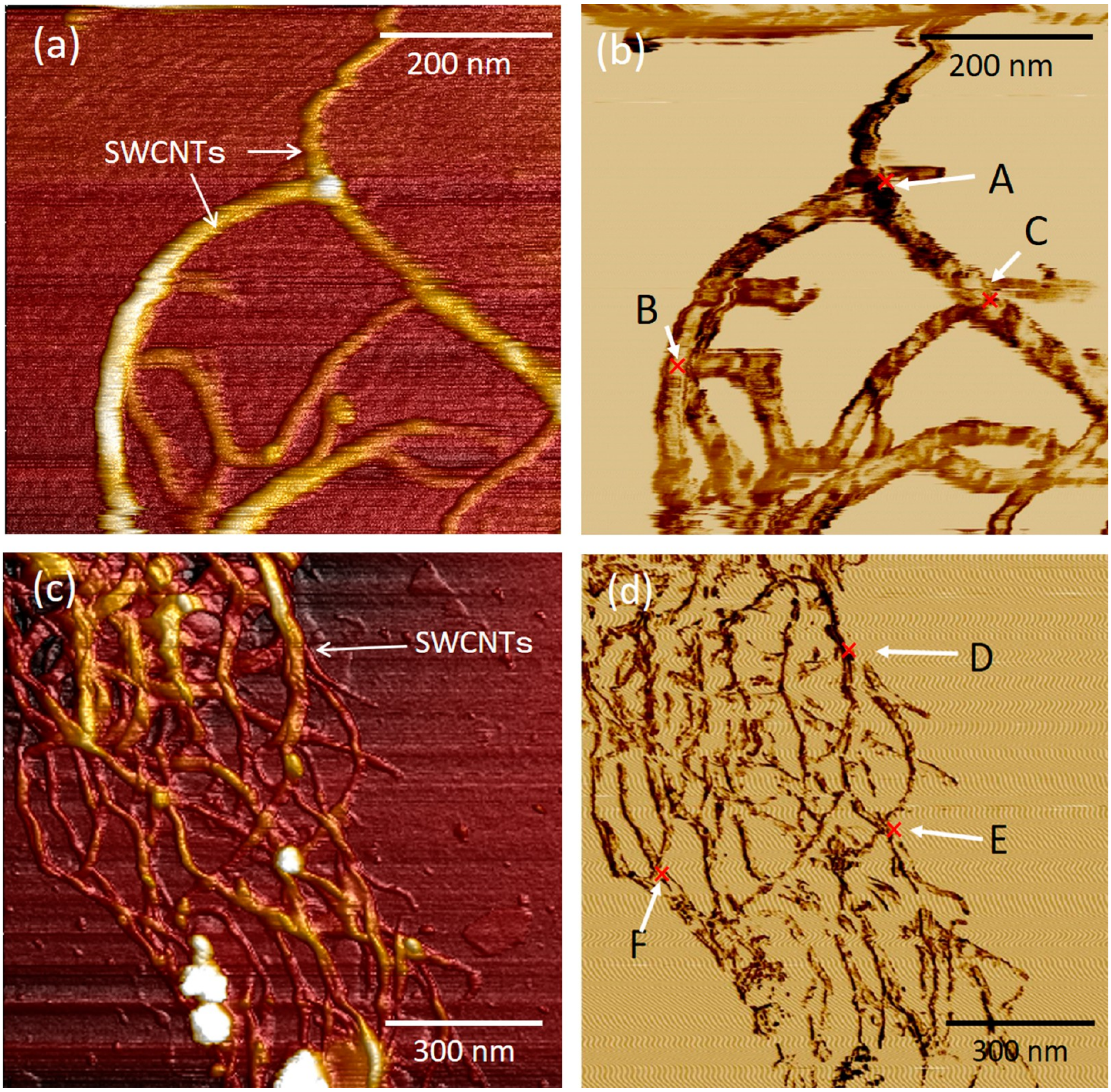

Figure 10. SPM images: (a, c) 3D images, and (b, d) current images obtained by applying voltage. (a, b) HC-SWCNTs dispersed on a Ta substrate. (c, d) SWCNTs with crystal defects on a Ta substrate.

through owing to the increased resistance and contact resistance of the CNTs themselves, and it can be assumed that the conductivity of the film is low.

■ CONCLUSIONS

In this study, a lightweight electromagnetic wave shield was successfully fabricated, using a formation technique based on a wet process to form the film into arbitrary shapes to be mounted on flexible devices for use in the IoT society, as a nanometer-sized or similarly sized electromagnetic wave shield material. Carbon nanomaterials of dielectric electromagnetic wave shields were used in this study. We have promoted research and development activities ranging from basic research on the synthesis of carbon nanomaterials to their applications and succeeded in developing synthesis methods for CNTs with desirable physical properties. Furthermore, for HC-SWCNTs, we have established a method of fabricating HC-SWCNTs from carbon materials synthesized from the arc discharge of a common carbon electrode. It has been confirmed that HC-SWCNTs with very high crystallinity, i.e., with almost no crystal defects in the carbon network comprising the CNTs, show physical properties close to those proposed theoretically. Using the thin-film formation technique to disperse CNTs, we have succeeded in forming a thin film that can shield devices against electromagnetic waves in the GHz band.

The conductive property of HC-SWCNTs was analyzed by SPM, and the dependence of the resistance property of SWCNTs on their crystallinity was examined. Using highly crystalline CNTs, including HC-SWCNTs, one can control the charge mobility of a thin film by controlling the density of HC-SWCNTs added to the thin film. From the results of this research, we have established a technology for implementing electronic wiring that maximizes the electric properties of HC-

https://doi.org/10.1021/acsomega.4c04285
ACS Omega 2024, 9, 29009−29016

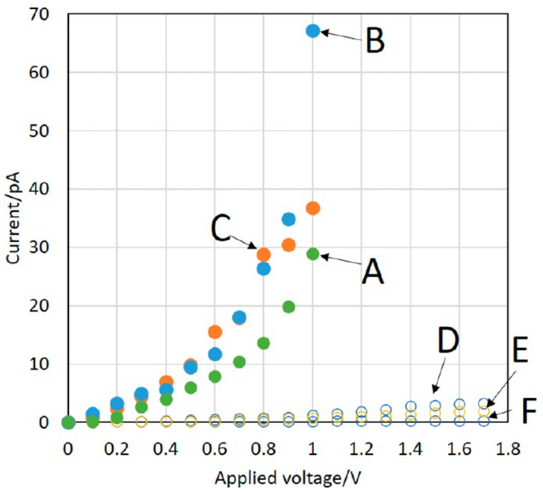

Figure 11. Current−voltage characteristics at arbitrary points A to F indicated by arrows in Figure 10b,d.

SWCNTs fabricated by a wet process. Moreover, we have fabricated a wet-type electromagnetic shield with high density and implementability while reducing the environmental impact of fabrication processes, thereby achieving a charge mobility close to the theoretical properties of CNTs. Further intensive research will be promoted to realize thin films.

To apply the dielectric properties of HC-SWCNTs, the technology for achieving the uniform dispersion of each material has been developed to form a thin film of an electromagnetic wave absorber with a controlled density of nanoparticles, and thin and lightweight HC-SWCNT composite-type electromagnetic wave absorbers are a clear departure from conventional heavy and bulky electromagnetic wave shields. We are convinced that the HC-SWCNT composite is useful for forming thin and lightweight electromagnetic wave absorbers.

■ ASSOCIATED CONTENT

Data Availability Statement

The data that support the findings of this study are available within the article.

■ AUTHOR INFORMATION

Corresponding Author

Norihiro Shimoi − *Department of Electrical and Electric Engineering, Tohoku Institute of Technology, Sendai, Miyagi 982-8577, Japan;* orcid.org/0000-0002-3787-3767; Email: n-shimoi@tohtech.ac.jp

Authors

Masae Komatsu − *Department of Electrical and Electric Engineering, Tohoku Institute of Technology, Sendai, Miyagi 982-8577, Japan*

Masayoshi Isago − *Department of Electrical and Electric Engineering, Tohoku Institute of Technology, Sendai, Miyagi 982-8577, Japan*

Complete contact information is available at: https://pubs.acs.org/10.1021/acsomega.4c04285

Notes

The authors declare no competing financial interest.

■ ACKNOWLEDGMENTS

This study was jointly conducted with DOWA Holdings Co., Ltd. The authors would like to thank the staff of DOWA for helpful discussions and proposals. Moreover, this study was conducted as a project consigned by the New Energy and Industrial Technology Development Organization and supported by JSPS KAKENHI Grant Number JP26220104. The authors would also like to express their sincere gratitude for the guidance received.

■ REFERENCES

(1) Al-Saleh, M. H.; Gelves, G. A.; Sundararaj, U. Copper nanowire/polystyrene nanocomposites: Lower percolation threshold and higher EMI shielding. *Plasma Sources Sci. Technol.* **2011**, *42* (1), 92−97.

(2) Kulal, S. R.; Khetre, S. S.; Jagdale, P. N.; Gurame, V. M.; Waghmode, D. P.; Kolekar, G. B.; Sabale, S. R.; Bamane, S. R. Synthesis of Dy doped Co−Zn ferrite by sol−gel auto combustion method and its characterization. *Mater. Lett.* **2012**, *84* (1), 169−172.

(3) Kadam, A. A.; Shinde, S. S.; Yadav, S. P.; Patil, P. S.; Rajpure, K. Y. Structural, morphological, electrical and magnetic properties of Dy doped Ni−Co substitutional spinel ferrite. *J. Magn. Magn. Mater.* **2013**, *329*, 59−64.

(4) Ameli, A.; Jung, P. U.; Park, C. B. Electrical properties and electromagnetic interference shielding effectiveness of polypropylene/carbon fiber composite foams. *Carbon* **2013**, *60*, 379−391.

(5) Ameli, A.; Jung, P. U.; Park, C. B. Through-plane electrical conductivity of injection-molded polypropylene/carbon-fiber composite foams. *Compos. Sci. Technol.* **2013**, *76* (4), 37−44.

(6) Tohji, K.; Goto, T.; Takahashi, H.; Shinoda, Y.; Shimizu, N.; Jeyadevan, B.; Matsuoka, I.; Saito, Y.; Kasuya, A.; Ohsuna, T.; Hiraga, K.; Nishina, Y. Purifying single-walled nanotubes. *Nature* **1996**, *383* (6602), 679−679.

(7) Iwata, S.; Sato, Y.; Nakai, K.; Ogura, S.; Okano, T.; Namura, M.; Kasuya, A.; Tohji, K.; Fukutani, K. Novel method to evaluate the carbon network of single-walled carbon nanotubes by hydrogen physisorption. *J. Phys. Chem. C* **2007**, *111*, 14937−14941.

(8) Karthikeyan, S.; Mahalingam, P.; Karthik, M. Large-scale synthesis of carbon nanotubes. *E-J. Chem.* **2009**, *6* (1), 1−12.

(9) Shimoi, N.; Kumon, S. Synthesis of high-purity and high-crystallinity single-walled carbon nanotubes homogeneously dispersed by wet process. *Adv. Powder Technol.* **2022**, *33* (11), No. 103825.

(10) Odom, T. W.; Huang, J. L.; Kim, P.; Lieber, C. M. Atomic structure and electronic properties of single-walled carbon nanotubes. *Nature* **1998**, *391*, 62−64.

(11) Martel, R.; Schmidt, T.; Shea, H. R.; Hertel, T.; Avouris, P. Single- and multi-wall carbon nanotube field-effect transistors. *Appl. Phys. Lett.* **1998**, *73*, 2447.

(12) Cao, Q.; Rogers, J. A. Ultrathin Films of Single-Walled Carbon Nanotubes for Electronics and Sensors: A Review of Fundamental and Applied Aspects. *Adv. Mater.* **2009**, *21* (1), 29−53.

(13) White, K. L.; Shuai, M.; Zhang, X.; Sue, H.-J.; Nishimura, R. Electrical conductivity of well-exfoliated single-walled carbon nanotubes. *Carbon* **2011**, *49* (15), 5124−5131.

(14) Shimoi, N.; Adriana, L. E.; Tanaka, Y.; Tohji, K. Properties of a field emission lighting plane employing highly crystalline single-walled carbon nanotubes fabricated by simple processes. *Carbon* **2013**, *65*, 228−235.

(15) Hou, P.-X.; Liu, C.; Cheng, H.-M. Purification of carbon nanotubes. *Carbon* **2008**, *46* (15), 2003−2015.

(16) Tanaka, H.; Goto, T.; Hamada, K.; Ohashi, K.; Osawa, T.; Sugime, H.; Noda, S. Safe and damage-less dry-purification of carbon nanotubes using $FeCl_3$ vapor. *Carbon* **2023**, *212*, No. 118171.

(17) Harutyunyan, A. R.; Awasthi, N.; Jiang, A.; Setyawan, W.; Mora, E.; Tokune, T.; Bolton, K.; Curtarolo, S. Reduced carbon solubility in Fe nano-clusters and implications for the growth of single-walled carbon nanotubes. *Phys. Rev. Lett.* **2008**, *100*, No. 195502.

(18) Yamabe, T.; Okahara, K.; Okada, M.; Tanaka, K. Electronic properties of bucky-tube model. *Synth. Met.* **1993**, *56* (2−3), 3142−3147.
(19) Jeong, S. H.; Kim, K. K.; Jeong, S. J.; An, K. H.; Lee, S. H.; Lee, Y. H. Optical absorption spectroscopy for determining carbon nanotube concentration in solution. *Synth. Met.* **2007**, *157* (13−15), 570−574.
(20) Hu, Y.; Li, D.-C.; Wu, L.; Yang, J.; Jian, X.; Bin, Y.-Z. Carbon nanotube buckypaper and buckypaper/polypropylene composites for high shielding effectiveness and absorption-dominated shielding material. *Compos. Sci. Technol.* **2019**, *181* (8), No. 107699.
(21) Dürkop, T.; Getty, S. A.; Cobas, E.; Fuhrer, M. S. Extraordinary Mobility in Semiconducting Carbon Nanotubes. *Nano Lett.* **2004**, *4* (1), 35−39.
(22) Dürkop, T.; Kim, B. M.; Fuhrer, M. S. Properties and applications of high-mobility semiconducting nanotubes. *J. Phys.: Condens. Matter* **2004**, *16*, R553−R580.
(23) Snow, E. S.; Campbell, P. M.; Ancona, M. G.; Novak, J. P. High-mobility carbon-nanotube thin-film transistors on a polymeric substrate. *Appl. Phys. Lett.* **2005**, *86*, No. 033105.
(24) Geim, A. K.; Novoselov, K. S. The rise of graphene. *Nat. Mater.* **2007**, *6* (3), 183−191.
(25) Abdalla, M.; Dean, D.; Adibempe, D.; Nyairo, E.; Robinson, P.; Thompson, G. The effect of interfacial chemistry on molecular mobility and morphology of multiwalled carbon nanotubes epoxy nanocomposite. *Polymer* **2007**, *48* (19), 5662−5670.
(26) Jousseaume, V.; Cuzzocrea, J.; Bernier, N.; Renard, V. T. Few graphene layers/carbon nanotube composites grown at complementary-metal-oxide-semiconductor compatible temperature. *Appl. Phys. Lett.* **2011**, *98*, 123103.
(27) Tans, S. J.; Verschueren, A. R. M.; Dekker, C. Room-temperature transistor based on a single carbon nanotube. *Nature* **1998**, *393*, 49−52.
(28) Snow, E. S.; Novak, J. P.; Campbell, P. M.; Park, D. Random networks of carbon nanotubes as an electronic material. *Appl. Phys. Lett.* **2003**, *82*, 2145−2147.
(29) Forrest, S. R. The path to ubiquitous and low-cost organic electronic appliances on plastic. *Nature* **2004**, *428*, 911−918.
(30) Moulton, B.; Zaworotko, M. J. From molecules to crystal engineering: Supramolecular isomerism and polymorphism in network solids. *Chem. Rev.* **2001**, *101* (6), 1629−1658.
(31) Wang, C.; Takei, K.; Takahashi, T.; Javey, A. Carbon nanotube electronics − moving forward. *Chem. Soc. Rev.* **2013**, *42*, 2592−2609.
(32) Nakamura, S.; Saito, K.; Kitagawa, G. S. Percolation Threshold of Carbon Black-Polyethylene Composites. *Jpn. J. Appl. Phys.* **1997**, *36* (8), 5163−5168.
(33) Bauhofer, W.; Kovacs, J. Z. A review and analysis of electrical percolation in carbon nanotube polymer composites. *Compos. Sci. Technol.* **2009**, *69* (10), 1486−1498.
(34) Jiang, J.-S.; Guo, R.-H.; Chiu, Y.-S.; Hua, C.-C. Percolation behaviors of model carbon black pastes. *Soft Matter* **2018**, *14*, 9786−9797.

https://doi.org/10.1021/acsomega.4c04285
ACS Omega 2024, 9, 29009−29016